Anal. Bioanal. Electrochem., Vol. 4, No. 6, 2012, 593 - 609

Analytical & Bioanalytical Electrochemistry

Full Paper

Electroplating and Corrosion study of Zn-Co, Zn-Fe and Zn-Co-Fe Alloys

Ramesh S. Bhat[1] and A. Chitaranjan Hegde[2,*]

[1]*Department of Chemistry, Nitte Mahalinga Adyanthaya Memorial Institution of Technology Nitte -574110, Karnataka, India*

[2]*Electrochemistry Research Laboratory, Department of Chemistry, National Institute of Technology Karnataka, Surathkal, Srinivasnagar-575025, India*

*Corresponding Author, Tel: +91-824-2474046 (Off), Fax: +91-824-2474033

E-mail: hegdeac@rediffmail.com

Received: 10 October 2012 / Accepted in revised form: 30 November 2012 / Published online: 30 December 2012

Abstract- Zn-Co, Zn-Fe and Zn-Co-Fe coatings were electrodeposited on mild steel from an acid sulphate bath, using thiamine hydrochloride (THC) and citric acid (CA) as additives. Bath constituents and operating parameters were optimized by standard Hull cell method, for peak performance of the coatings against corrosion. The effect of current density (c.d.), pH on the deposit characters, such as corrosion resistance, hardness, thickness, partial current density and CCE were studied and discussed. Corrosion resistances were evaluated by Potentiodynamic polarization and electrochemical impedance spectroscopic (EIS) method. Corrosion resistance of the Zn-Co-Fe coating under optimal c.d. (3.0 A dm^{-2}) was found due to its inherent high dielectric barrier, evidenced impedance signals. High partial current density for zinc in Zn-Co-Fe alloy coating supports the possibility of a synergistic catalytic effect of Co on Fe and vice versa. X-ray diffraction study clearly indicates that a drastic change in corrosion resistance of ternary alloy is due to the change in the phase structure of the coatings, compared to binary alloys. Surface morphology and composition of the coatings were examined by using Scanning Electron Microscopy (SEM), interfaced with Energy Dispersive X-ray Analysis (EDXA) facility, respectively.

Key words- Zn-Fe Group Metal Alloys, Corrosion Behavior, Partial Current Density, SEM, XRD

1. INTRODUCTION

Electroplating of Zn-M alloys (where M=Ni, Co and Fe) is of highest interest in industrial level due to genuine reason of their best corrosion resistance. The characteristics of Zn-M alloys, such as anticorrosive properties, increased glossiness, hardness, capacity of hydrogen embrittlement, are better than those of pure zinc [1,2]. Corrosion resistance, along with other mechanical and physical properties of the coatings such as hardness and ductility depends on the specific procedure used for its preparation. It has been shown that the corrosion resistance of electrodeposited Zn-Ni alloy is better corrosion resistant than for pure zinc of equal thickness [3]. It was observed that the addition of Co to Zn-Ni alloy has led to the formations of ternary Zn-Ni-Co alloys, which improves drastically the appearance and its corrosion resistance [4,5]. Better corrosion resistance of Zn-M alloys is believed due to the introduction of slightly nobler metal into the crystal lattice and depends practically on the percentage of more noble metal in the deposit. Tafel extrapolation method, electrochemical impedance spectroscopic (EIS) technique is particularly valuable to investigate the corrosion mechanism [6,7]. Furthermore, Albalat et al. found that the presence of particular additives in the electrodeposition bath improved the surface homogeneity, which leads to better corrosion resistance, even for an alloy with low metal content [8].

The electrodeposition of Zn-Fe group metal alloys is classified by Brenner [9] as an anomalous codeposition, where zinc is the less noble metal, deposits preferably with respect to the more noble metal. Because of this fact the more noble metal content in Zn-M alloys produced from aqueous plating bath is usually low. Although this phenomenon has been known since 1907, the codeposition mechanisms of zinc and metal are not well understood [10,11]. There are some propositions to explain the anomalous codeposition of Zn-M alloys. Dahms and Croll [12] suggested that the formation of metal hydroxide located in the vicinity of electrode hindered deposition of more noble metal. The hydroxides formed oscillated under galvanostatic conditions and resulted in non laminated structures. It was, however, later that anomalous codeposition occurred even at low current densities, where hydroxide formation is unable to cause large alkalinization effects [13]. Another proposition is based on the under potential deposition of less noble metal on the cathode surface suppresses the deposition of more noble metal [14,15]. The term under deposition potential is used for the deposition of metal species on a foreign substrate in a potential which is more positive than the equilibrium potential of the bulk deposit. Matlosz [16] uses two-step reactions involving adsorbed monovalent intermediate ions for both electrodeposition of iron and cobalt, as single metals, and combines the two to develop a model for codeposition. A main contribution of this model is the inclusion of hydrogen adsorption and its effects on electrodeposition. Baldwin. et al. [17] concluded that deposition of iron group metals leads to a reduction of the reaction rate of the nobler metals and an increase of the reaction rate of the less noble metal compared to single metal deposition.

Cadmium plating has been extensively used as a corrosion resistant coating on hard steel for various applications. Zamanzadeh et al., [18] found that deposits of cadmium reduced the hydrogen permeation on iron. Kim et al., [19] developed an alkaline electrodeposition process to deposit good quality Zn-Ni-Cd deposits with high wt.% of Ni and Zn contents. The resultant Zn-Ni-Cd deposits have excellent corrosion resistance and barrier properties. Crystalline Zn-Ni and Zn-Fe alloy deposits can turn into amorphous by P incorporation. The amorphous characteristics have been observed for alloys with more than 10% P content [20,21]. Abou Krishna et al. [22] have studied extensively the electrodeposition of ternary Zn-Ni-Fe alloy and, compared the results with that of Zn, Ni, Fe and Zn-Ni alloy deposition. They showed that increase in corrosion resistance of ternary alloy deposits is not only attributed to the formation of γ-Ni_2Zn_{11} phase, but also to codeposition of Fe. Ternary Zn-Ni-Fe alloy coatings were found to a better surface appearance than binary Zn-Ni alloy coatings, even without adding any brighteners. The micro hardness of the thin films was found to increase with increasing iron content in the deposit [23]. Further, it was observed that ternary Zn-Ni-Co alloys are characterized by enhanced corrosion resistance, compared to the binary Zn-Ni and Zn-Co alloys [5,24].

The objective of the present work is to propose stable sulfate baths for electrodeposition of Zn-Co, Zn-Fe and Zn-Co-Fe alloys on mild steel and to compare their corrosion performance. The effect of bath composition and operating parameters on composition and morphology of the deposits were studied. Factors responsible for improved corrosion resistance of ternary alloy compared to binary alloys were analyzed and discussed. The XRD analysis was carried out to identify the phase structures of the deposits.

2. EXPERIMENTAL

Electroplating solutions were prepared from LR grade chemicals and distilled water. All depositions were carried out at 30 ^oC and plating baths were adjusted to pH 3.0-4.0 with dilute solutions of sulfuric acid. Solution pH was monitored frequently and adjusted when necessary. Mild steel panels were smoothly polished and cleaned by anodic and cathodic electrolysis for 2 min in an aqueous solution of NaOH 35 g/L and Na_2CO_3 25 g/L at 6 A dm^{-2}. Samples were then neutralized in a 2 N HCl solution and rinsed with distilled water and were plated at required c.d. After deposition, the cathode were washed with tap water and rinsed with distilled water and dried. A PVC cell of 250 mL in capacity were used for electroplating with cathode - anode space of about 5 cm. Polished mild steel cathode panels of standard size and pure zinc anode were used for Hull cell study. The corrosion behaviors of electrodeposits were studied by DC/AC electrochemical techniques using VersaSTAT3 Potentiostat/Galvanostat (Princeton Applied Research) with built-in software. The reference electrode was Ag/AgCl/Cl-sat. and a platinum wire was counter electrode. The corrosion

behaviors of electroplated coatings were studied in 5% NaCl solution by potentiodynamic polarization method at the scan rate of 1 mV s^{-1}. Impedance behavior of Zn-Co, Zn-Fe and Zn-Co-Fe alloy deposits were studied by Nyquist plot in the frequency range from 100 kHz to 20 mHz. To determine the compositions of the coatings, the electrodeposits were stripped in 1:3 HCl solutions and wt. %Co and Fe were estimated calorimetrically [25]. The thickness of the deposits was calculated from Faradays law. The validity of measured thickness was cross examined using digital thickness tester (Coatmeasure M&C, ISO-17025/2005). The hardness of the deposit (~20 μm thickness) was measured by Vickers method using Micro Hardness Tester (CLEMEX). The cathode current efficiency of deposition was determined by knowing the mass and composition of the deposit [10]. The phase structure of the alloys, corresponding to different current densities were analyzed using X-ray Diffractometer (Bruker AXS), using Cu Kα- radiation, (λ 1.5405=A0, 30 kV). The microstructures of the deposits were examined by Scanning Electron Microscopy (SEM, Model JSM-6380 LA from JEOL, Japan).

3. RESULTS AND DISCUSSION

3.1. Hull cell studies

The bath composition and operating parameters of Zn-Co and Zn-Fe and Zn-Co-Fe baths have been optimized by conventional Hull cell method [26] at 1.0 A cell current, at temperature 30 ^{o}C. Varieties of deposits having grayish white/bright/mirror bright/porous black appearance were obtained over the wide range of current density of 1.0-5.0 A dm^{-2}. Effect of each bath constituents on Hull cell panels were examined in terms of their appearance and surface morphology. The composition and operating parameters of optimal bath is given in Table 1.

3.2. Effect of current density

3.2.1. Wt. % metal in the deposit

The effect of c.d. on wt. %Co and wt. %Fe were studied using optimal bath. It was found that c.d. plays an important role on both appearance and corrosion performance of deposit. Increase of wt. %Co and Fe with increase in current densities and bath follows anomalous codeposition over the entire range of 1.0 A dm^{-2} - 5.0 A dm^{-2}. Both the baths have produced semi bright deposit at low c.d. side and a porous bright deposit at high c.d. The brightness of the deposit was found to be due to thiamine hydrochloride (THC) and citric acid (CA) in the bath. The variation of wt. % of M with c.d. in binary and ternary alloys is shown in Table 2.

A sound deposit of Zn-Fe alloy was found at 3.0 A dm^{-2} with about 3.62% Fe. The increase of wt. %Fe in the deposit at low c.d. side is attributed to the tendency of the system to follows normal type with preferential deposition of Fe. For the optimized Zn-Co bath wt.

%Co obtained in the deposit was varied from 0.39% to 1.08% for different c.d.'s. A sound deposit of Zn-Co alloy was found at 4.0 A dm^{-2} with about 1.02% Co. A small increase in the wt % of more noble metals was observed in ternary alloy system with increased corrosion resistance as shown in Table 2. At optimal condition, the ternary alloy showed 6.1 wt. %Fe and 0.62 wt. %Co (against 3.62 wt. %Fe and 1.02 wt. %Co in binary alloy coating) in the deposit. It may be observed that a small increase in the noble metal content has brought a significant change in the intrinsic electrical properties of the deposit, and hence its corrosion resistance.

Table 1. Composition and operating parameter of optimal bath for electrodeposition of bright Zn-Fe, Zn-Co and Zn-Fe-Co alloy on mild steel

Bath composition (g L^{-1})	Zn-Fe	Zn-Co	Zn-Fe-Co
Zinc sulphate	50.0	50.0	70.0
Ferric sulphate Cobaltous	20.0	0.00	20.0
sulphate	0.00	15.0	25.0
Citric acid	4.0	4.0	4.0
Sodium acetate Thiamine	60.0	60.0	60.0
hydrochloride	0.5	0.5	0.5

Table 2. Effect of CCE (%) and wt.% of noble metal in binary and ternary alloy deposits obtained at different current densities

c.d (A dm^{-2})	Zn-Fe		Zn-Co		Zn-Co-Fe		
	wt.% of Fe	CCE (%)	wt.% of Co	CCE (%)	wt.% of Fe	wt.% of Co	CCE (%)
1.0	2.1	90.6	0.39	96.1	4.3	0.36	93.2
2.0	2.7	91.2	0.46	97.3	5.1	0.40	94.6
3.0	3.6	92.6	0.6	98.6	6.1	0.62	97.7
4.0	4.9	90.7	1.06	99	6.4	1.02	96.9
5.0	6.8	87.3	1.08	93.7	6.8	1.04	95.3

3.2.2. Cathode current efficienc

The cathode current efficiency in electroplating or cathode efficiency is the percentage of the total current usefully employed for the cathodic deposition of the metal. This can be calculated from the relationship:

$$\text{Efficiency} = \frac{\text{Measured mass gain}}{\text{Theoritical mass gain}} \times 100$$

Theoretical mass gain can be calculated from Faradays law by accurately measuring the quantity of the electricity that flows through the solution for known time. CCE increases with current density to an optimal level and then decreases in case of binary and ternary alloy coatings as shown in Table 2.

3.2.3. Thickness of deposit

The thickness of the deposit was found to increase substantially with c. d. in both binary and ternary alloys as shown in Table 3, 4 and Table 5. The linear dependency of thickness of the deposit with current density may be explained by the fact that, at very high current density, adsorbed metal hydroxide film at cathode (due to local decrease of pH by evolution of hydrogen) likely to get occluded in the crystal lattice of deposits. Bath temperature also has prominent role on the thickness, composition and appearance of the deposit as exhibited by other Zn-Fe group metal alloys.

Table 3. Corrosion parameters of Zn-Fe alloy deposits obtained under different current densities using aerated 5% NaCl

c.d (A dm^{-2})	VHN	*t* (μm)	E_{corr}V *vs.* Ag/AgCl/$Cl_{sat.}$	i_{corr} (μA cm^{-2})	CR×10^{-2} (mm y^{-1})
1.0	143.0	7.9	-1.259	12.26	18.2
2.0	167.0	9.6	-1.240	6.06	8.8
3.0	179.0	12.5	-1.290	1.55	2.2
4.0	193.0	16.7	-1.234	3.97	5.8
5.0	197.0	18.9	-1.259	8.02	11.7

3.2.4. Hardness of deposit

The hardness of deposit was found to increase with wt. %Fe, Co in binary and ternary alloy in the deposit as shown in Table 3, 4 and Table 5. It may ascribed by the inherent high density cobalt, iron (d_{Zn}=7.14 g cm^{-3} and d_{Co} =8.90 g cm^{-3}) in the deposit. But at very high c.d. the coating was very thick and porous with decreased hardness. Thick and porous deposit at high c.d. is due to metal hydroxide formation caused by rapid evolution of hydrogen during plating.

Table 4. Corrosion parameters of Zn-Co alloy deposits obtained under different current densities using aerated 5% NaCl

c.d ($A\ dm^{-2}$)	VHN	*t* (μm)	E_{corr} V *vs.* $Ag/AgCl/Cl_{sat.}$	i_{corr} ($\mu A\ cm^{-2}$)	CR×10^{-2} ($mm\ y^{-1}$)
1.0	152.0	8.2	-1.295	6.57	9.6
2.0	185.0	10.6	-1.302	5.76	8.5
3.0	195.0	13.5	-1.300	5.22	7.7
4.0	259.0	17.7	-1.233	4.83	7.1
5.0	286.0	20.9	-1.335	5.36	7.8

Table 5. Corrosion parameters of Zn-Co-Fe alloy deposits obtained under different current densities using aerated 5% NaCl

c.d ($A\ dm^{-2}$)	VHN	*t* (μm)	E_{corr} V *vs.* $Ag/AgCl/Cl_{sat.}$	i_{corr} ($\mu A cm^{-2}$)	CR×10^{-2} ($mm\ y^{-1}$)
1.0	156	7.9	-1.279	2.16	3.1
2.0	162	12.5	-1.313	0.34	0.5
3.0	194	14.9	-1.316	0.15	0.2
4.0	210	24.3	-1.382	1.05	1.5
5.0	219	25.2	-1.320	1.37	1.9

3.3. Corrosion Study

3.3.1. Tafel Study

Electroplated specimens were subjected to corrosion study in aerated 5% NaCl solution and experimental data of the binary Zn-Fe and Zn-Co alloy are given in Table 3 & 4. Table 5 shows the corrosion properties of ternary alloy. Corrosion rates of the deposits were determined by Tafel's extrapolation method. The observed corrosion potential, E_{corr} corrosion current density, i_{corr} and corrosion rate, CR at different current densities are shown in Table 3 and 4 and 5. The E_{corr} values of Tafel plots indicate that the corrosion rate is controlled more

by cathodic reaction. Tafel behavior of Zn-Fe, Zn-Co and Zn-Co-Fe alloys deposited under optimal conditions are shown Fig. 1. It may be observed that i_{corr} value of ternary alloy is much less compared to other two binary Zn-Co and Zn-Fe alloys. Zn-Co-Fe alloy at the current density of 3.0 A dm^{-2} with 6.1% Fe and 0.62% Co shows the least corrosion rate of 0.22×10^{-2} mm y^{-1} which is about ~10 times less compared to Zn-Fe (2.26×10^{-2} mm y^{-1} at 3.0 A dm^{-2}) and ~30 times less in case of Zn-Co (7.08×10^{-2} mm y^{-1} at 4.0 A dm^{-2}) alloy.

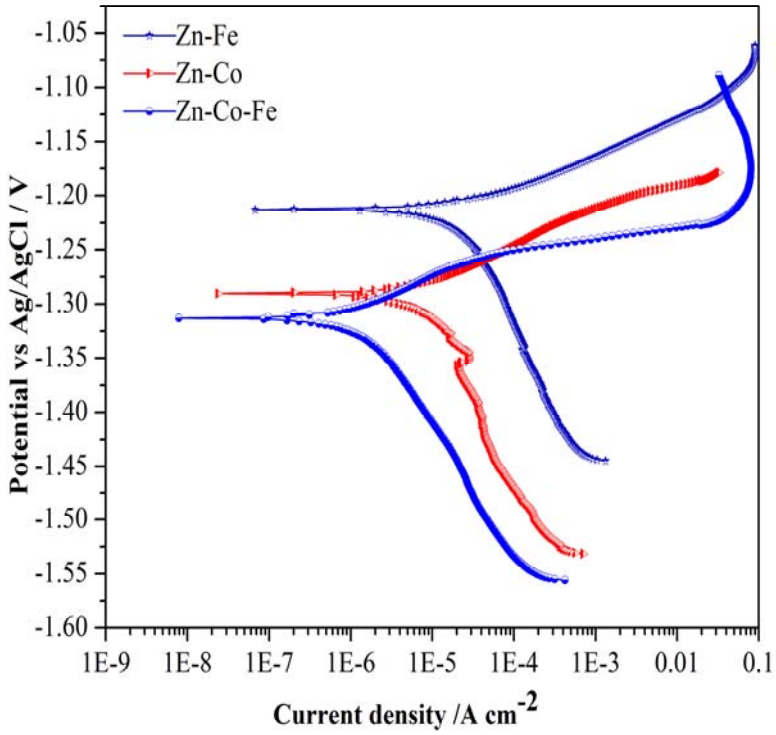

Fig. 1. Tafel plots for Zn-Co, Zn-Fe and Zn-Co-Fe alloy deposits obtained at optimized current densities from the optimal bath at scan rate of 1 mVs^{-1}

3.3.2. Electrochemical impedance spectroscopy (EIS)

EIS spectra were used to evaluate the barrier properties of the coatings and to determine the polarization resistance. The superior corrosion resistance in Zn-M alloy coatings can be explained by the barrier protection mechanism theory. Electrochemical impedance spectra of Zn-Co, Zn-Fe and Zn-Co-Fe alloys deposited under optimal conditions are shown Fig. 2. The solution resistance *R*s was nearly identical in all cases as the same bath chemistry and cell configuration were used. The significantly higher impedance and larger diameter of (unfinished) semicircle in the case of the ternary alloy reflect its higher corrosion resistance, which is consistent with a change in the film (coating) capacitance *Cf*. The capacitive impedance at high frequencies is well related to the thickness and the dielectric constant of

the film. No diffusion-limited process, in the form of Warburg impedance, was evident. It was found that radius of the semicircle in ternary Zn-Co-Fe alloy is high compared to that of binary Zn-Fe and Zn-Co alloys. The increased corrosion resistance is attributed to the semiconductor behavior of thin films at the interface of alloy deposit and corroding medium.

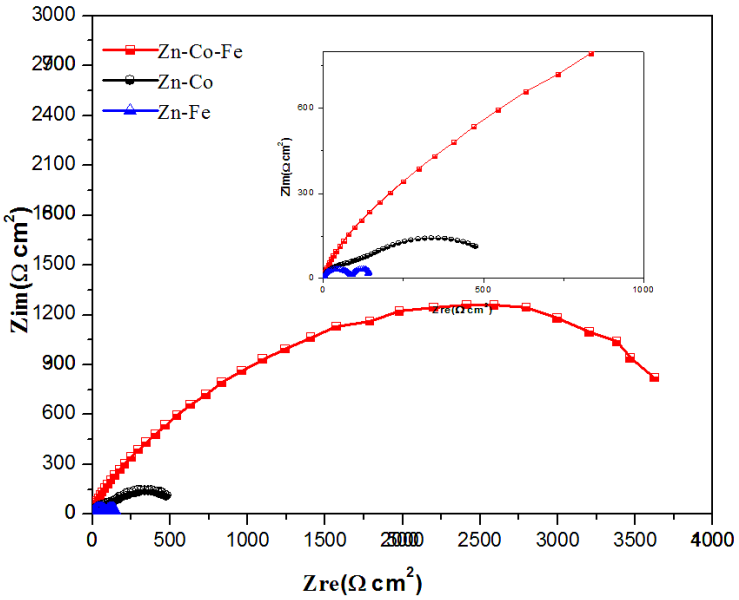

Fig. 2. Comparison of Electrochemical Impedance Spectra of Zn-Co, Zn-Fe and Zn-Co-Fe alloy coatings obtained at optimal current density's from the optimal bath (high frequency limit is shown in the inset)

3.4. Cyclic polarization study

In the forward scanning, the value of current density went through from negative to positive side, which shows that the oxidizing reaction of passivation film occurred with increasing potential. After the passivation breakdown the protective films to start the pitting. The current density in the passive state is generally very low compared with that in the active state. The stability of passivation depends on the predominant cathodic process (hydrogen evolution, reduction oxygen and reduction metal ions). During backward scanning, the value of current density went through from positive to negative, indicating that reduction reaction of the high valence oxide in the passivation film occurred with the falling potential. In the Fig. 3 shows the current density of backward scanning is higher than that of the forward scanning, indicating that the dissolving of oxides had occurred and the current density of backward scanning was lower than that of forward scanning, which shows that metal could form protective passive film below this value. In the Fig. 3 showed that the current density of backward scanning was higher than that of the forward scanning in the potential range from 0.25 V to - 0.7 V in relation with the breakdown of the air formed oxide layer, and it was

lower than that of forward scanning in the potential range from -0.7 V to -0.9 V due to the formation of corrosion products. This supported the corrosion process of Zn-Co-Fe coating on mild steel as explained in the earlier sections.

3.5. Circuit fitment for optimal conditions

Electrochemical reactions consist of electron transfer at the electrode surface. These reactions mainly involve electrolyte resistance, adsorption of electroactive species, charge transfer at the electrode surface, and mass transfer from the bulk solution to the electrode surface. The better corrosion resistance of ternary coating, in relation to binary alloy may reasoned by the electrochemical process taking place at the interface of the substrate. i.e. between mild steel and corrosion medium. The process taking place at the interface may be represented by an electric circuit composed of resistance R, capacitance C , Inductance I and constant phase elements (CPE), combined in parallel or in series. In EIS technique, it is common to plot the data as imaginary impedance versus real impedance with provision to distinguish the polarization resistance contribution, R_p from the solution resistance, R_s. These plots are often called Nyquist diagrams of circuit fitments.

The experimental impedance data of Zn-Co, Zn-Fe and Zn-Co-Fe coatings were fitted to an appropriate equivalent circuit using *ZSimpWin 3.21* software, interfaced with potentiostat/ galvanostat. A close agreement was found between measured and calculated values of circuit elements, as shown in Fig. 4. It may be observed that binary $(Zn\text{-}Co)_{4.0}$ exhibited the corrosion circuit, consisting of many circuit elements like L, C, R Q, and W without CPE's and circuit can be represented as: (LR(C(R(Q(R(RW)))))) and $(Zn\text{-}Fe)_{3.0}$ exhibited two capacitive loops, corresponding to two CPE's, with less R_p, and high C values. The simulated circuit can be represented is as: LR(QR(CR)(LR)(CR)).

In case of ternary Zn-Co-Fe alloy coating, electrical equivalent circuit composed of resistive/capacitive elements in series and parallel, with circuit description code R(C(R(QR)))(CR) was proposed. It consisting of many circuit elements like C, Q and R, without CPE's similar to Zn-Co coating with high R_p, and high C values. It implies that increased corrosion resistance of the ternary alloy coatings is due to distortion of the capacitance, caused by the electrode surface roughness or distribution/accumulation of charge carriers.

3.6. Effect of partial current densities on the deposit

Zn-Co-Fe bath produced semi-bright deposits at low c.d. and porous bright deposits at high current density. A sound deposit of Zn-Co-Fe alloy containing 0.62 wt. % Co and 6.1 wt. % of Fe was obtained at i=3.0 A dm^{-2}. The partial deposition current densities were calculated from the mass gained and the chemical composition of the deposit, using the equation:

$$i_i = \frac{w}{At} \times \frac{c_i n_i F}{M_i}$$

where i_i is the partial current density of element i (A dm^{-2}) and A is the surface area of the cathode (cm^2). Fig. 5 shows the dependence of the partial current densities of Zn, Fe and Co on the applied current density. The partial current densities increased as the applied current density was increased. It is also evident that in Zn-Co-Fe alloy system the partial current density of Zn is higher than those of the Fe and Co metals. This supports the possibility of a synergistic catalytic effect of Co on Fe and vice versa.

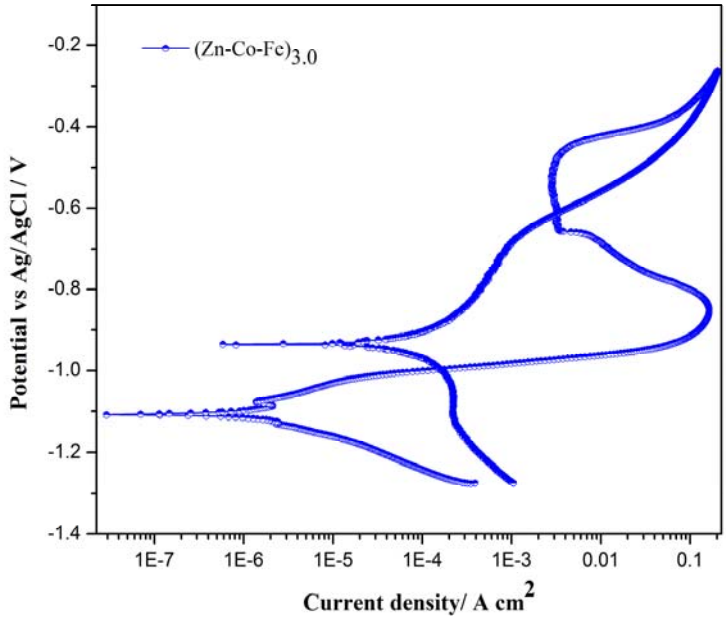

Fig. 3. Potentiodynamic cyclic polarization data display for electrodeposited Zn-Co-Fe alloy coatings from optimal bath at 3.0 A dm^{-2}

3.7. Surface study

The microstructure of deposits, observed by SEM, difference in the uniformity was observed with the increase in the quantity of more noble metal. Fig. 6(a) and (b) shows the surface morphology of the Zn-Fe and Zn-Co deposits as observed by SEM. This shows a smooth non granular deposit. As shown in Fig. 6(a) the morphology of the deposits with low cobalt content is granular and more isotropic in shape. Similar type of morphology was observed for Zn-Fe deposit with the high iron content. Fig. 6(c) shows the SEM image of ternary Zn-Fe-Co deposit. A smooth granular uniform morphology was observed in ternary

alloy deposit, which is due to the higher percentage of more noble metal in the deposit. EDX analysis was carried out to investigate the metal percentage in the deposit. Distinct peaks for metals are observed by EDX analysis of the deposit which confirms the formation of alloy, and their compositions are quantified (Fig. 8). The results obtained with EDX analysis and colorimetric determination is same within the experimental error.

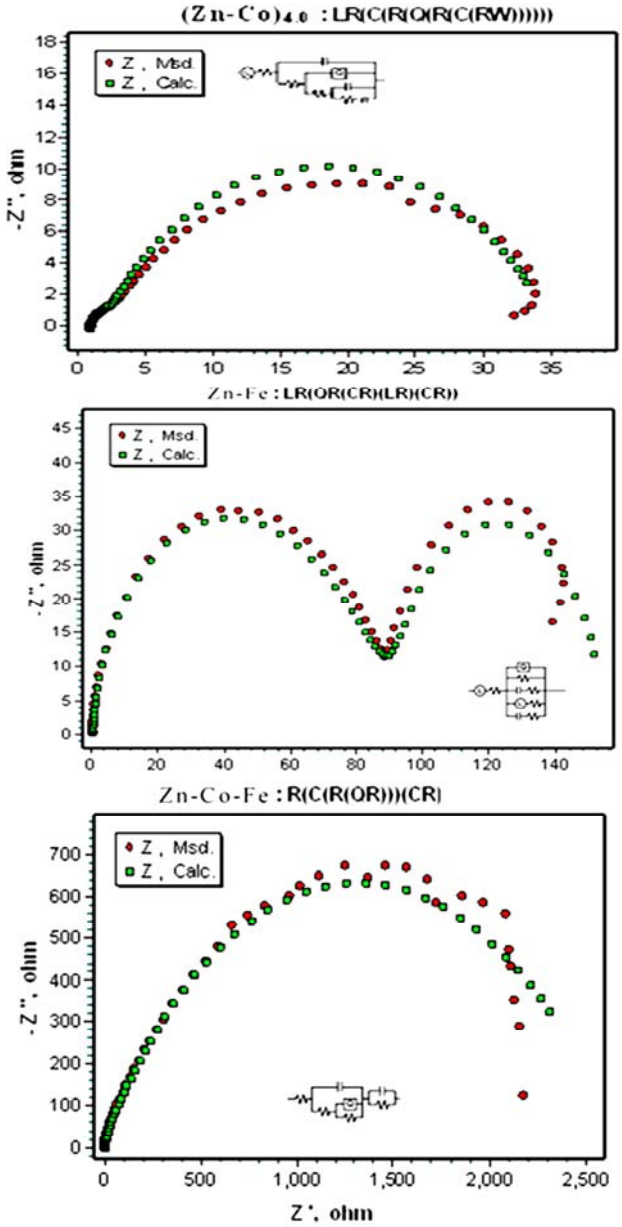

Fig. 4. Equivalent circuit fitment for corrosion circuit, corresponding to monolayer of Zn-Co, Zn-Fe and Zn-Co-Fe coatings, under optimal current densities

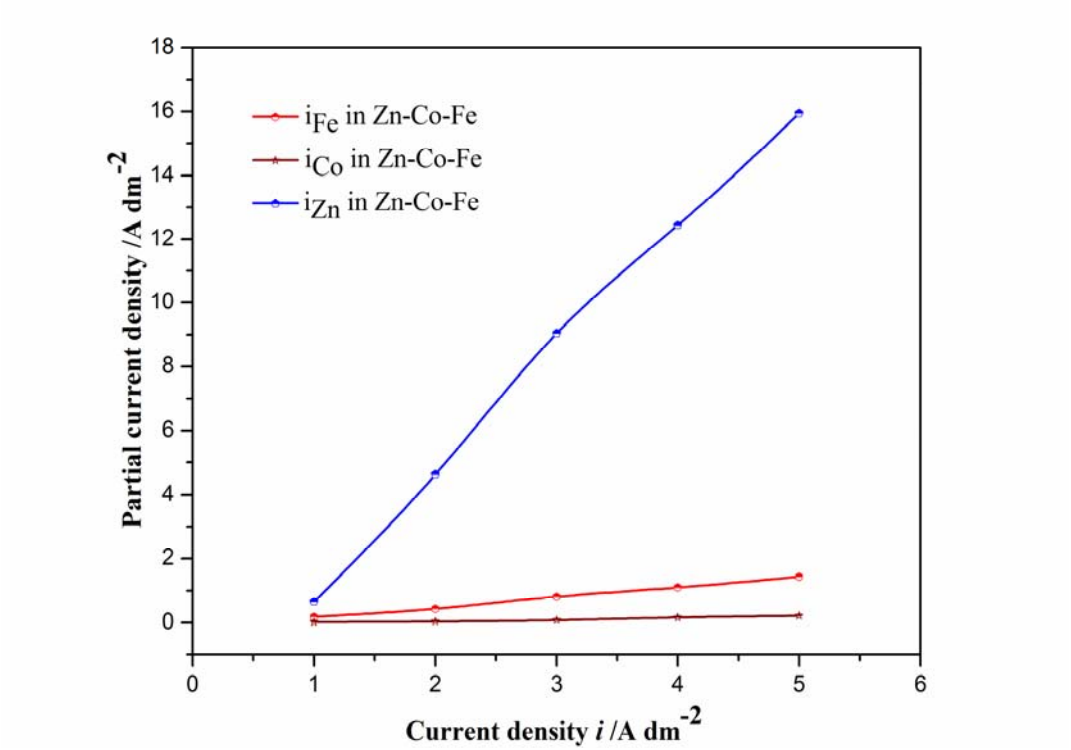

Fig. 5. In Zn-Co-Fe alloy coating, the dependence of the partial current densities of Zn, Fe and Co on the applied current densities.

3.8. X-Ray Diffraction Study

Fig. 7 shows the XRD spectra for Zn-Co, Zn-Fe and Zn-Co-Fe coatings on mild steel. The Zn (110) reflection was the highest of zinc, in Zn-Co and Zn-Fe coating indicating preferred orientation of this phase [27]. The spectrum of the Zn-Co-Fe coating was much different. The intensity of Zn (101) became the strongest. This change in phase content could be reflected by the different appearance in SEM images (Fig. 6). It may be observed that the intensity of the peak corresponding Zn (100) and Zn (110), Zn (101) increases progressively in binary and ternary alloy coatings at optimized c.d. Thus X-ray diffraction study clearly indicates that a drastic change in corrosion resistance of Zn-Co-Fe coating is the consequent of change in the phase structures of the coatings.

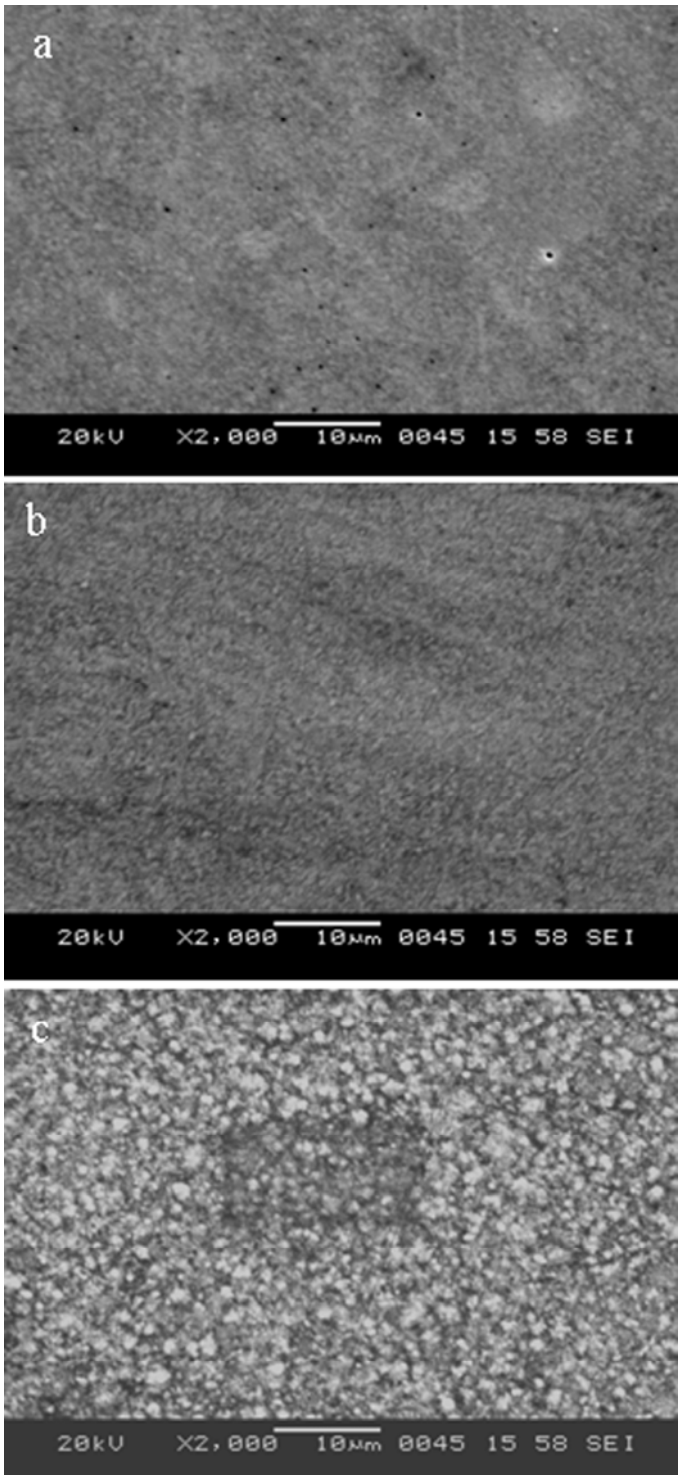

Fig. 6. SEM image of Zn-Co, Zn-Fe and Zn-Co-Fe deposit at optimal current densities (a) 4.0 A dm^{-2}, (b) 3.0 A dm^{-2}, and (c) 3.0 A dm^{-2}

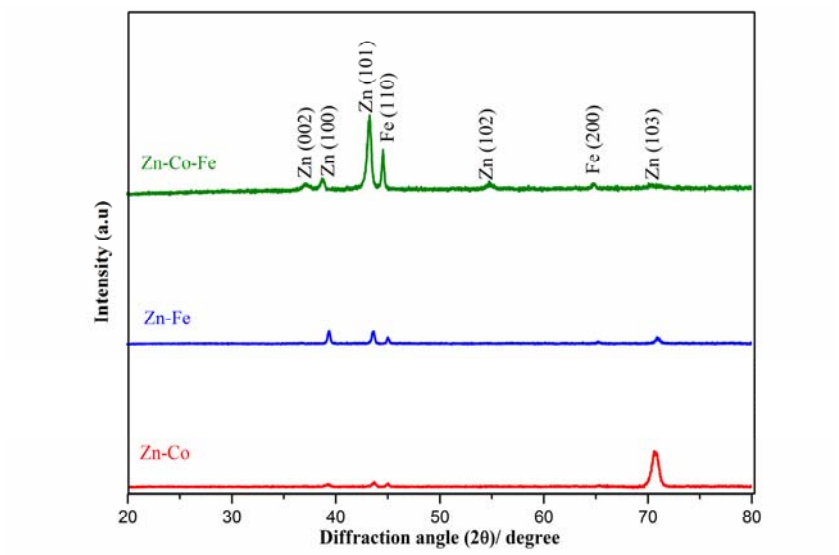

Fig. 7. X-ray diffraction profiles of electrodeposits obtained on mild steel from optimized bath at optimal current densities, as mentioned on the plot

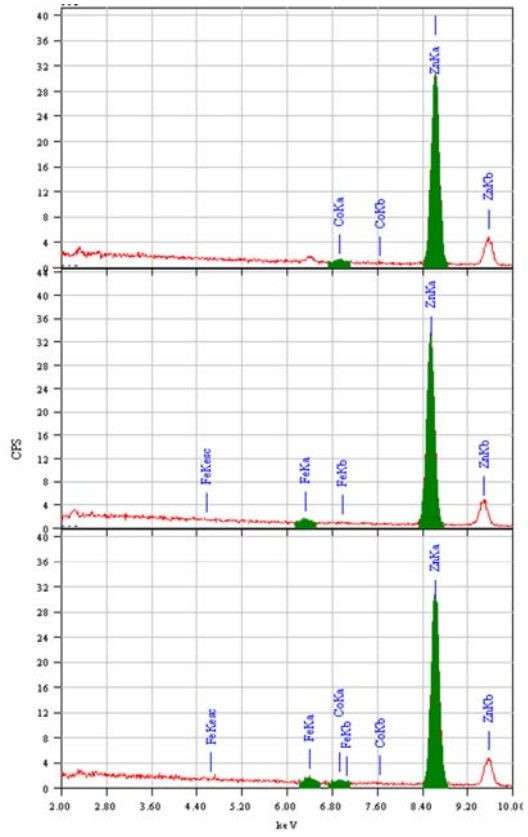

Fig. 8. EDX Spectra of Zn-Co-Fe, Zn-Fe and Zn-Co alloy deposit at optimal current densities

4. CONCLUSIONS

The following conclusions were drawn from the present study:

1. The stable binary and ternary baths for electroplating of bright Zn-Co, Zn-Fe and Zn-Co-Fe alloy over mild steel have been proposed. Under worked conditions, the bath followed anomalous codeposition with preferential deposition of less noble metal.
2. Zn-Co alloy, having about 1.06 wt. % Co deposited at i=4.0 A dm^{-2}; and Zn-Fe alloy, having about 3.6 wt. %Fe deposited at i=3.0 A dm^{-2} wt. % Co, and Zn-Co-Fe alloy, having about 0.62 wt.% Co and 6.1 wt.% Fe deposited at i=3.0 A dm^{-2} ,were highly corrosion resistant.
3. The cyclic polarization study showed the improved corrosion resistance is due to barrier effect of oxide layer and corrosion products.
4. Corrosion study showed that Zn-Co-Fe alloy deposit is about 30 and 10 times more corrosion resistant than Zn-Co and Zn-Fe alloy deposits, respectively.
5. Partial c.d. study revealed that in both binary and ternary alloy coating systems, the rate of Zn deposition is heavily influenced by mass-transport limitation at high applied current densities, while the rates of Co and Fe deposition were not.
6. The SEM images of electroplates confirmed that superior corrosion resistance is due to improved homogeneity of the deposits.
7. X-ray diffraction study clearly indicates that a drastic change in corrosion resistance of Zn-Co-Fe alloy coating is the consequent of change in the phase structures of the coatings.

REFERENCES

[1] R. Fratesi, G. Roventi, and G. Giuliani, J. App. Electrochem. 27 (1997) 1088.
[2] Z. L. Wang, Y. X. Yang, and Y. R. Chen, J. Corr. Sci. Eng. 7 (2005) 8.
[3] D. E. Hall, Plat. Surf. Finish. 70 (1983) 59.
[4] M. M. Younan, and T. Oki, J. Appl. Electrochem. 26 (1996) 537.
[5] M. M. Younan, J. Appl. Electrochem. 30 (2000) 55.
[6] H. Bai, and F. Wang, J. Mater. Sci. Technol. 23 (2007) 541.
[7] L. Felloni , R. Fratesi, E. Quadrini, and G, Roventi, J. Appl. Electrochem. 17 (1987) 574.
[8] R. Albalat, E. Gomez , C. Muller, M. Sarret, and E. Valles, J. Appl. Electrochem. 20 (1990) 635.
[9] A. Brenner, Electrodeposition of alloys, Academic Press, New Yark 2 (1963) 194.
[10] E. P. Shoch, and A. Hirsch, J. Am. Chem. Soc. 29 (1907) 314.
[11] F. B. Growcock, and R. J. Jasinski, J. Electrochem. Soc. 136 (1989) 2310.

[12] H. Dhams, and I. M. Croll, J. Electrochem. Soc. 112 (1965) 771.
[13] H. Yan, J. Downes, P. J. Boden, and S. J. Harris, J. Electrochem. Soc. 143 (1996) 1577.
[14] J. Horkans, J. Electrochem. Soc. 128 (1981) 45.
[15] S. Swathirajan, J. Electrochem. Soc. 133 (1986) 671.
[16] M. Matlosz, J. Electrochem. Soc. 140 (1993) 2272.
[17] K. R. Baldwin and C. J. E. Smith, Trans IMF. 74 (1996) 202.
[18] M. Zamanzadeh, A. Allam, C. Kato, B. Ateya, and H. W. Pickering, J. Electrochem. Soc. 129 (1982) 284.
[19] H. Kim, B. N. Popov, and K. S. Chen, J. Electrochem. Soc. 150 (2003) 81.
[20] K. Shidharan, and K. Sheppard, J. Appl. Electrochem. 27 (1997) 1198.
[21] M. Bouanani, F. Cherkaoui, and R. Fratesi, J. Appl. Electrochem. 29 (1999) 637.
[22] M. M. Abou-Krishna, F. H. Assaf, and S. A. El-Naby, J. Solid. State .Electrochem. 13 (2009) 879.
[23] M. M. Younan, R. Ichino, and T. Oki, Metal. Finish. 94 (1996) 40.
[24] A. Petrauskas, L. Grinceviciene, A. Cesuniene, and R. Juskenas, Electrochimca. Acta 51 (2006) 6135.
[25] A. I. Vogel, Quantitative Inorganic Analysis, (Longmans Green & Co., London) (1951) 194.
[26] N. Kanani, Electroplating: Basic Principles, Processes and Practice, (Elsevier Ltd, Berlin, Germany) 2006.
[27] N. Eliaz, K. Venkatakrishna, and A. Chitharanjan Hegde, Surf. Coat. Technol. 205 (2010) 1969